Simulation of actual evapotranspiration and evaluation of three complementary relationships in three parallel river basins

Yongshan Jiang (jiangys.19s@igsnrr.ac.cn)

Institute of Geographic Sciences and Natural Resources Research CAS: Institute of Geographic Sciences and Natural Resources Research Chinese Academy of Sciences

Zhaofei Liu

Institute of Geographic Sciences and Natural Resources Research Chinese Academy of Sciences https://orcid.org/0000-0003-4556-6641

Research Article

Keywords: Generalized complementary relationship, Hydrological budget balance, Actual evapotranspiration, Climate change

Posted Date: June 22nd, 2022

DOI: https://doi.org/10.21203/rs.3.rs-1641674/v1

Abstract

Based on observed precipitation and runoff data, monthly actual evapotranspiration (ET_a) was calculated by the hydrological budget balance method in the three parallel river basins. The performance of three developed complementary relationship methods, the nonlinear advection-aridity (non-AA) method, generalized complementary relationship method (B2015), and sigmoid generalized complementary function (H2018), on simulating ET_a were evaluated. The evaluation results showed that three methods were able to accurately simulate monthly ET_a series. The Nash-Sutcliffe efficiency coefficient between the monthly ET_a simulated by the non-AA, B2015, and H2018 methods and the water-balance-derived ET_a were 0.74, 0.78, and 0.79, respectively. The correlation coefficient were 0.84, 0.89, and 0.90, respectively. And the root mean square errors were 10.76 mm mon^{-1}, 10.01 mm mon^{-1}, and 9.78 mm mon^{-1}, respectively. The ET_a increased spatially from upstream region to downstream region at catchment scale. Annual ET_a simulated by the non-AA, B2015 and H2018 models showed significant increasing trends during 1956–2018 in the basins, with the increasing magnitudes of 1.53 mm/a, 1.66 mm/a and 1.47 mm/a, respectively. Research on the influence between meteorological factors and ET_a showed that there was a positive correlation between ET_a and precipitation, temperature, wind and sunshine hours, with the average correlation coefficient of 0.40、0.64、0.63 and 0.72, respectively. The value between ET_a and relative humidity was − 0.38. The ET_a in the basins was highly sensitive to temperature, wind speed and sunshine hours, with the average sensitivity coefficient of 0.26, 0.21 and 0.27, respectively. And moderately sensitive to relative humidity, with a sensitivity of -0.18.

1. Introduction

Actual evapotranspiration (ET_a) plays a crucial role in the global water and energy cycles. ET_a and runoff account for 59% and 41% of land surface precipitation, respectively (Oki and Kanae 2006). And the solar radiation energy absorbed by land surface exceeds 50% is used for ET_a (Trenberth et al. 2009). ET_a can reflect the regional changes of land surface energy and hydrological budgets. Analyses of trends of ET_a are greatly significant for understanding climate change and its impacts at regional scales. Accurate simulation of ET_a is crucial for the management and planning of water resources, forestry, and agricultural irrigation (Maes et al. 2012; Farahani et al. 2007; Fisher et al. 2017).

Obtaining ET_a is a challenging task because of its complex interactions across the soil-plant-atmosphere continuum (Katul et al. 2012). ET_a can be accurately monitored by a wide variety of ground measurements such as lysimeters, energy balance Bowen ratio, and eddy covariance (Allen et al. 2011). However, estimation of large-scale, long-term ET_a remains difficult since these techniques typically cover short periods with limited spatial extent (Ma and Szilagyi 2019). And most ET_a methods require a significant number of soil and vegetation-related parameters as inputs (Masson et al. 2003), thus leading to data complexity and additional uncertainties.

There are several methods can estimate ET_a by using only routine meteorological observations data (Chen et al. 2020; Fan et al. 2018; McMahon et al. 2013). Among them, Bouchet (1963) proposed a complementary relationship (CR) which had been proven to be a feasible and efficient approach (Xu and Singh 2005; Hobbins et al. 2001). The original complementary principle based a linear CR between ET_a, potential evapotranspiration (ET_p), and wet environment evapotranspiration (ET_w), in which ET_a and ET_p depart from ET_w in opposite directions when the land surface is drying from completely wet conditions with a constant energy input (Brutsaert 2015; Zhou et al. 2020). Several methods based on the CR had been proposed such as Advection-Aridity (Brutsaert and Strick 1979), CRAE (Morton 1983), and Granger-Gray (Granger and Gray 1989) methods. And they had been extensively used for obtaining long-term regional ET_a (Jian et al. 2018; Szilagyi et al. 2009).

However, in recent years, many studies had shown that it was difficult for ET_a and ET_p to satisfy the completely symmetrical CR. Brutsaert (2015) formulated a more general and nonlinear version of the CR which defined as "the generalized complementary relationship" by generalizing the CR to a fourth-order polynomial function between ET_a/ET_{Pen} and ET_w/ET_{Pen}. Han et al. (2018) combing a sigmoid form of the generalized complementary function into the traditional AA method to represent the relationship between ET_a and ET_p by considering boundary conditions for extremely arid and completely wet environments. Szilagyi et al. (2017) proposed a calibration-free nonlinear CR method with more appropriate physical constraints which built on the latest researches of the nonlinear formulation by Brutsaert (2015) and Crago et al. (2016). The most prominent advantage in the method is that it determines the parameter of the Priestley-Taylor coefficient (Priestley and Taylor 1972) from temperature and humidity data over wet areas.

A wide range of studies have investigated the spatiotemporal pattern of ET_a at regional scales (Gao et al. 2007; Liu et al. 2019; Xu et al. 2021; Yang et al. 2021). However, there are relatively few studies on ET_a changes and evaluation of the developed CR methods in three parallel river basins. The three parallel river basins are characterized as unique dry-hot valley. The Nu River and Lancang River, which are located in the region, are the upper reaches of the international Salween River and Mekong River, respectively. It includes semi-arid, semi-humid, and humid regions. Investigation on spatial pattern and temporal change of ET_a in this region would attract extensive concern (Sabo et al. 2017). Their water fluctuation could not only affect the water availability, the ecological environment, and food security but also pose enormous challenges to transboundary water utilization and allocation (Fan and He 2015). Therefore, the research on trends of hydrological variables in the basins have attracted extensive attention.

In this study, the water balance-based ET (WB_ET) series was used to evaluate the accuracy of the CR based ET (CR_ET) in three parallel river basins. The objectives of this study were to: (1) simulating ET_a by the corrected hydrologic budget balance method; (2) evaluating the accuracy of three

developed CR methods in simulating monthly ET_a; (3) detecting trends of ET_a during the past six decades, and quantifying sensitivity of climate factors to regional ET_a changes.

2. Materials And Methods

2.1 Study Area

The three parallel river basins include a series of parallel north-south mountain ranges in southwest China. The study area includes the Nu River, Lancang River, and Jinsha River basins above the Daojieba, Yunjinghong and Shigu stations, respectively. The Nu River and Lancang River are the upstream of the Salween River and Mekong River, respectively, which are important international rivers. The terrain of this region is complex and changeable, characterized by deep V-shaped valley with fast velocity of surface and subsurface runoff. The climate in the region varied significantly from the north to south. The upstream region belongs to a plateau climate of semi-arid region with low temperature and little precipitation. The midstream and downstream regions are located in the subtropical and tropical climate zones of semi-humid and humid regions. In general, mean annual precipitation in the three parallel river basins ranges from 150 mm yr^{-1} to 1500 mm yr^{-1}, and heavy rains are concentrated in the wet season (May to October). Mean annual air temperature is between 10°C and 30°C. Annual ET ranges from 50 mm yr^{-1} in the north to 1500 mm yr^{-1} in the south. The wet season ET accounts for 85% of the annual ET.

Figure 1 Location of each catchment, hydrological stations, and weather stations

2.2 Data

(1) Observed meteorological data

Observed daily meteorological data for the period from 1956 to 2018 at 35 stations in and near the study area were obtained from the China Meteorological Administration (http://data.cma.cn/). The data includes precipitation, air temperature, wind speed, relative humidity, and sunshine hours. The monthly and annual series were calculated from the daily observed data series. The area weight of each station was used to calculate the regional average value. The area weights were calculated based on the Tyson polygon method.

(2) Observed hydrological data

Observed runoff data from nine hydrological stations on the main stream of the HDM region were used in this study. Each hydrological station represented the main stream control station of the upstream, midstream and downstream regions of the Nu River, Lancang River, and Jinsha River, respectively (Fig. 1). The information on the nine hydrological sites were listed in Table 1. Data were obtained from the China Hydrological Yearbook.

Table 1
Observed runoff data from nine hydrological stations

	Hydrological station	Longitude	Latitude	Catchment area (km^2)	Temporal coverage
NRB	Jiayuqiao	96.24	30.87	68384	1956–2000, 2007–2018
	Gongshan	98.68	27.73	101146	1956–2000
	Daojieba	98.88	24.98	110224	1956–2000
LCRB	Changdu	97.17	31.15	53800	1956–2000, 2007–2018
	Jiuzhou	99.22	25.79	88051	1956–2000
	Yunjinghong	100.78	22.03	115894	1956–2000
JSRB	Zhimenda	97.22	33.03	137704	1956–1987, 2007–2018
	Batang	99.02	29.83	187873	1956–1987, 2007–2018
	Shigu	99.93	26.9	214184	1956–1987, 2007–2018

Table 1. Observed runoff data from nine hydrological stations

2.3 Simulation of ET_a

2.3.1 Hydrological budget balance method

ET_a was simulated by the hydrological budget balance method at basin scales (Liu et al. 2014; 2019; Wan et al. 2015). In a basin, the hydrological budget balance equation could be expressed as:

$$ET_i^{WB} = P_i - R_i - \Delta W \quad (1)$$

where P and R are the basin-wide totals of precipitation (mm) and the net stream flow at the basin outlet (mm), respectively, ΔW is the change in terrestrial water storage including the surface, subsurface, and ground water changes (mm) at a monthly or annual scale.

At the simulation of monthly ET_a, ΔW is usually negligible in many studies, which assumes precipitation (evaporation) is the only source (loss) of water in the basin (Hobbins et al., 2001; Zhang et al., 2012). However, the hydrological budget balance may not close when ΔW is neglected under changing climate and anthropogenic interferences such as water diversion, reservoir regulation, and agricultural irrigation (Liu et al., 2016). In this study, we defined (*P-R*) as the biased $ET^{WB}{}_{\text{biased}}$ relative to the reference ET^{WB}. The $ET^{WB}{}_{\text{biased}}$ can be corrected based on ET^{WB} measured during the same period at the monthly scale through a two-step bias correction method (BCM, Li et al., 2014). Firstly, at each basin, the monthly ET^{WB} and $ET^{WB}{}_{\text{biased}}$ series were fitted separately using a gamma distribution. This has been shown as an effective method for modeling the probability distribution of ET_a (Liu et al. 2016). Water-balance-derived ET_a was used for trends detection of ET_a in the NRB and LCRB during 1956–2018 by the rank-based nonparametric Mann-Kendall test in seasonal and annual time series.

2.3.2 Nonlinear AA method

Brutsaert and Strick (1979) proposed the AA method,

$ET_a{}^{AA} = 2ET_w - ET_p$ (2)

Kahler and Brutsaert (2006) pointed out that the assumed symmetric nature of the CR becomes asymmetric when used with evaporation pan data. This meant that the change in the apparent potential evaporation, as the environment dries from an initially wet condition, will be larger than the corresponding change in ET_a. Therefore, the AA method had since evolved to adopt the asymmetric CR (Brutsaert and Parlange 1998; Szilagyi 2007).

$ET_p - ET_w = b\,(ET_w - ET_a)$ (3)

where b is another constant of proportionality. Rearrangement of (3) leads to

$$ET_a = \frac{1+b}{b}ET_w - \frac{1}{b}ET_p$$

4

In non-AA method, ET_p and ET_w are denoted by the Penman (1948) equation (E_{Pen}) and the Priestley-Taylor (1972) equation, respectively.

$$ET_w = \alpha ET_{rad} = \alpha\frac{\Delta}{\Delta+\gamma}(R_n - G)$$

5

$$ET_p = ET_{rad} + ET_{aero} = \frac{\Delta}{\Delta+\gamma}\left(R_n - G\right) + \frac{\gamma}{\Delta+\gamma}f\left(u_2\right)(e_s - e_a)$$

6

Normalized by E_{Pen}, the non-AA method can be expressed as a linear function (Han et al. 2008):

$$ET_a = \frac{1+b}{b}ET_w - \frac{1}{b}ET_p$$

7

where E_{rad} and E_{aero} are the radiation and aerodynamic terms for the Penman equation, respectively (mm/day); α is an empirical coefficient; Δ is the slope of the saturation vapor pressure curve at air temperature (hPa/°C); γ is the psychrometric constant (hPa/°C); R_n is the net radiation near the surface (mm/day); G is the soil heat flux; $f(u_z)$ is the wind function, which is calculated by Penman's wind function (Penman, 1948), that is, $f(u2) = 0.26(1 + 0.54u2)$, where u_2 is the wind speeds at 2 m heights (m/s); e_s is the vapor pressure of the air (hPa); and e_a is the saturation vapor pressure at air temperature (hPa). All these variables are calculated by the method recommended by the Food and Agriculture Organization (FAO) of the United Nations (Allen 2000).

2.3.3 B2015 method

Brutsaert (2015) generalized the CR to a fourth-order polynomial function between ET_a/ET_{Pen} and ET_w/ET_{Pen}, the application of which still requires specifying the methods of ET_{Pen} and ET_w. Considering the relationship with non-AA approach, this new polynomial function is regarded as the generalized nonlinear advection_aridity method (B2015) and has the same variables as the non-AA function (Crago et al. 2016; Ma et al. 2019), that is:

$$ET_a^{B2015} = \left(\frac{ET_w}{ET_p}\right)^2 [(2-c)ET_p - (1-2c)ET_w - c\frac{ET_w^2}{ET_p}]$$

8

where c is thought to be zero under usual situations (Brutsaert, 2015). Thus, a fixed c = 0 and calibrated parameter α of the B2015 have been adopted for daily (Aietal.,2017; Brutsaert et al., 2017; Hu et al., 2018; Zhang et al., 2017), annual, and multi-year scales (Liu et al., 2016). The Eq. (8) could be represented as:

$$ET_a = \left(\frac{ET_w}{ET_p}\right)^2 (2ET_p - ET_w)$$

9

2.3.4 H2018 method

Han et al. (2018) developed a nonlinear CR method (Han et al. 2012) by introducing minimum (X_{min}) and maximum (X_{max}) limits to ET_{rad}/ET_{Pen} (Han and Tian 2018). This sigmoid generalized complementary function (H2018) can be written as:

$$\frac{ET^{H2018}}{E_{Pen}} = \frac{1}{1 + m\left(\frac{x_{max} - x}{x - x_{min}}\right)^n}$$

10

where x_{min} and x_{max} corresponding to the minimum and maximum values of ET_{rad}/ET_{Pen}; x is defined as the ratio of ET_{rad} to ET_{Pen}; and m and n are constants. The H2018 exhibits a three-stage pattern, and ET_a/ET_{Pen} increases approximately linearly with ET_{rad}/ET_{Pen} during the middle stage in environments that are neither too dry nor too wet. By making a first order Taylor expansion of the H2018 at ET_a/ET_{Pen} = 0.5 equal to the linear AA function, parameters m and n can be transferred from α and b^{-1}:

$$\begin{cases} n = \frac{4\alpha(1+b^{-1})(x_{0.5} - x_{min})(x_{max} - x_{0.5})}{(x_{max} - x_{min})} \\ m = \left(\frac{x_{0.5} - x_{min}}{x_{max} - x_{0.5}}\right)^n \end{cases}$$

11

where $x_{0.5}$= $(0.5 + b^{-1})/(\alpha(1 + b^{-1}))$ is the value of E_{rad}/E_{Pen} corresponding to ET_a/E_{Pen}= 0.5. The linear AA function can be regarded as a special case of the H2018 (Han and Tian 2018), for which x_{min}= 0 and x_{max}= 1 have been suggested for a daily scale because the function and simulated results are not sensitive to x_{min} and x_{max}.

2.4 Evaluation criteria

The performance of monthly ET data sets was evaluated by WB_ET. The evaluation criteria included relative error (RE), Pearson correlation coefficient (cc), root mean square error (RMSE), and Nash-Sutcliffe efficiency (NSE) (Jiang and Liu 2021).

$$\mathrm{RE} = \frac{x(i) - y(i)}{y(i)} \times 100$$

12

$$\mathrm{cc} = \frac{\sum_{i=1}^{n}\left[x(i) - \bar{x}\right][y(i) - \bar{y}]}{\sqrt{\sum_{i=1}^{n}[x(i) - \bar{x}]^2}\sqrt{\sum_{i=1}^{n}[y(i) - \bar{y}]^2}}$$

13

$$\mathrm{RMSE} = \sqrt{\frac{1}{n}\sum_{i=1}^{n}[x(i) - y(i)]^2}$$

14

$$\mathrm{NSE} = 1 - \frac{\sum_{i=1}^{n}[x(i) - y(i)]^2}{\sum_{i=1}^{n}[y(i) - \bar{y}]^2}$$

15

where x(i) and y(i) are the model and observed variable at *i*-time step, $\bar{x}$ and $\bar{y}$ are the model and observed mean, respectively; n is the total number of observations; α is the ratio between the variance of the model variable and observed variable and β is the ratio between the mean of the model variable and observed variable.

2.5 Influence of meteorological factors on $\mathbf{ET_a}$

Meteorological factors with strongly physically correlation with ET_a were selected for analysis, including precipitation, air temperature, relative humidity, wind speed, and sunshine hours (Li et al. 2014; Valipour 2015). The sensitivity coefficient (McCuen 1974) of meteorological factors to ET_a could be expressed as follows,

$$S_{V_i} = \frac{\Delta ET}{\Delta V_i}\frac{V_i}{ET}$$

16

where ET and ΔET are the daily ET_a and daily variation, respectively; and V_i and ΔVi are the daily meteorological factor values and daily variation, respectively. Under the condition that the variable of a single meteorological factor varies by ± 10%, the sensitivity coefficient of ET_a to each meteorological factor was calculated in turn.

3. Results

3.1 The performance of three developed CR methods in simulating monthly $\mathbf{ET_a}$

In this study, the ranges of parameter α and b^{-1} for the non-AA method were [0.89, 1.14] and [0.16, 0.77], respectively. The ranges of parameters α of the B2015 was [0.94, 1.13] with an average value of 1.03; For the H2018, the range of parameter α was [1.01,1.14] with an average value of 1.05, and the ranges of parameter b^{-1} was [0.18, 1.08].

The performance of the non-AA, B2015, and H2018 methods in simulating monthly ET_a in the three parallel river basins were compared (Table 2). The discrepancies among the three developed methods for ET_a estimation was small. The RE between the monthly ET_a simulated by the non-AA, B2015, and H2018 methods and the water balance-derived ET_a were 3.8%, 2.3%, and 2.4%, respectively. The NSE of three developed methods were 0.74, 0.78, and 0.79, respectively. The R-square were 0.84, 0.89, and 0.90, respectively. And the RMSE were 10.76 mm mon^{-1}, 10.01 mm mon^{-1}, and 9.78 mm mon^{-1}, respectively. Overall, the H2018 performed better than the B2015 and non-AA methods. The performance of three developed CR methods in simulating wet season ET_a was generally similar with that of annual ET_a. It showed a relatively poor performance in simulating dry season ET_a, with the mean NSE lower than 0.6 for non-AA method. However, the RE were less than 10%, indicating that the methods were able to accurately simulate the average value. In general, the developed CR methods were able to simulate ET_a with a high accuracy at the annual and wet season scales in the three parallel river basins. The simulation accuracy of the JSRB was slightly higher in terms of evaluation criteria.

Table 2
Evaluation results of three developed CR methods in simulating monthly ET_a

Model	Basin		NSE			cc			RMSE		
			Annual	or frequency of 19.4% was g Dry	Wet	Annual	Dry	Wet	Annual	Dry	Wet
non-AA	NRB	NU	0.74	0.53	0.72	0.81	0.66	0.86	9.59	4.41	8.36
		NM	0.72	0.59	0.74	0.79	0.68	0.85	9.78	7.15	8.84
		ND	0.75	0.66	0.76	0.85	0.71	0.87	13.93	7.98	11.78
	LCRB	LCU	0.68	0.54	0.67	0.79	0.63	0.84	10.45	6.16	9.68
		LCM	0.79	0.61	0.80	0.83	0.67	0.77	11.68	6.91	9.45
		LCD	0.82	0.50	0.83	0.89	0.72	0.89	13.45	9.81	12.90
	JSRB	JSU	0.70	0.59	0.68	0.73	0.64	0.80	8.02	3.71	7.84
		JSM	0.70	0.59	0.77	0.86	0.68	0.82	9.43	5.16	8.45
		JSD	0.76	0.65	0.79	0.87	0.68	0.82	10.51	6.59	9.81
	Mean		0.74	0.58	0.75	0.84	0.67	0.84	10.76	6.43	9.68
B2015	NRB	NU	0.78	0.54	0.75	0.86	0.68	0.92	8.93	4.11	7.78
		NM	0.75	0.60	0.78	0.89	0.71	0.90	9.10	6.66	8.22
		ND	0.79	0.68	0.80	0.90	0.74	0.93	12.95	7.43	10.95
	LCRB	LCU	0.70	0.55	0.69	0.84	0.65	0.89	9.72	5.74	9.01
		LCM	0.84	0.63	0.85	0.88	0.69	0.81	10.86	6.44	8.79
		LCD	0.87	0.51	0.88	0.95	0.75	0.95	12.51	9.13	12.00
	JSRB	JSU	0.73	0.60	0.71	0.84	0.66	0.85	7.47	3.47	7.29
		JSM	0.73	0.61	0.82	0.91	0.70	0.87	8.77	4.81	7.86
		JSD	0.80	0.67	0.84	0.93	0.71	0.87	9.77	6.14	9.13
	Mean		0.78	0.60	0.79	0.89	0.70	0.89	10.01	5.99	9.00
H2018	NRB	NU	0.79	0.56	0.77	0.87	0.70	0.93	8.72	4.00	7.60
		NM	0.77	0.62	0.79	0.90	0.73	0.91	8.89	6.50	8.03
		ND	0.80	0.70	0.81	0.91	0.76	0.94	12.67	7.25	10.71
	LCRB	LCU	0.72	0.57	0.71	0.85	0.67	0.90	9.50	5.60	8.80
		LCM	0.85	0.65	0.86	0.89	0.71	0.82	10.62	6.28	8.59
		LCD	0.88	0.53	0.89	0.96	0.77	0.96	12.23	8.92	11.73
	JSRB	JSU	0.75	0.62	0.73	0.85	0.68	0.86	7.29	3.37	7.12
		JSM	0.75	0.63	0.83	0.92	0.72	0.88	8.57	4.69	7.68
		JSD	0.81	0.69	0.85	0.94	0.73	0.88	9.55	5.99	8.92
	Mean		0.79	0.62	0.80	0.90	0.72	0.90	9.78	5.84	8.80

Table 2. Evaluation results of three developed CR methods in simulating monthly ET_a

Frequency distributions of the RE for the non-AA, B2015 and H2018 methods in simulating annual, wet and dry seasons ET_a were shown in Fig. 2. In general, the frequency of the RE of developed CR methods exhibited a normal distribution. In term of the frequency distribution of the H2018 method, more than 95.2% of the errors were between − 25% and 25%. Among them, the error frequency between − 5% and 5% was the highest, with the value of 30.1%. The frequency distribution of wet season was consistent with that of annual series. An 85.7% margin of error was 255 between − 25% and 25%. The error frequency was the highest between − 5% and 5%, with the value of 30.6%. The frequency distribution of the RE of dry season ET_a was not consistent with that of wet season. More than 52.4% of errors were between − 15% and 20%. Among them, the highest between 5% and 10% with the value of 9.5%.

The error frequency of 19.4% was greater than 50%, which was much higher than that of 2.4% in annual and rainy seasons. The RE was slightly higher in dry season in terms of frequency distribution. The frequency distribution of the RE for non-AA and B2015 were basically the same as those of H2018. For example, more than 90% of the errors were between − 25% and 25%, and the error frequency was the highest between − 5% and 5% with the value of 33.3%. However, there were some inconsistencies. For example, the B2015 method had a better simulation effect in dry season. More than 71.4% of the errors distributed between − 25% and 25%. The error frequency was the highest between − 10% and − 5% with the value of 14.3%.

Figure 2 Frequency distributions of the relative error for the non-AA, B2015 and H2018 methods

3.2 Trends of ET_a, precipitation, and runoff in the NRB and LCRB

The spatial pattern of annual WB_ET in the three parallel river basins was increased spatially from upstream region (143 mm/a) to downstream region (707 mm/a) at catchment scale. The wet season ET accounted for 70–90% of annual ET.

The spatial trend of evapotranspiration simulated by the CR_ET showed that a notable lower value in the northern site and higher value in the southern site at three temporal scales, which was similar to the findings for WB_ET. Among them, the simulation results of the H2018 model show that the ET_a was the lowest in the upstream region of the Jinsha River basin, with a multi-year average ET_a of 205 mm yr^{-1}, while the highest value in the downstream region of Lancang River basin, with the ET_a of 1385 mm yr^{-1}.

Trends of annual ET estimated from the WB_ET in the three parallel river basins exhibited an increasing trend during 1960–2018 in the NRB, LCRB, and JSRB, with the magnitude being 1.41 mm/a, 0.60 mm/a, and 1.37 mm/a, respectively. It showed a decreasing trend in the upstream region. The decreasing trend was significantly (significance level of 0.05, the same below) at the NU and LCU. The significant increasing trends were detected at the downstream region. Trends of ET in the dry and wet seasons (not shown) were similar to that in annual scale. The dry season ET decreased significantly at the LCU and JSU, while the wet season ET decreased significantly in the NU.

Figure 3 Variation trend of ET_a of (a) interannual (b) dry season (c) wet season in the three parallel rivers region basins

Trends of ET estimated by the CR method at the site scale were generally consistent with that derived by the WB method at the catchment scale (Fig. 4). ET exhibited an increasing trend during 1960–2018 in the NRB, LCRB, and JSRB, with the magnitude being 1.53 mm/a, 0.66 mm/a, and 1.47 mm/a, respectively. Where a decreasing trend in the upstream region was observed. An increasing trend of the annual CR_ET estimated by CR model was showed in half of sites (17/35), of which was concentrated in the downstream region. The trends of dry season and wet season CR_ET series (not shown) were consistent with that of annual CR_ET series. The trend type for CR_ET was mainly non-significant decrease (14/35), followed by non-significant increase (11/35). The dry and wet season ET series were basically consistent with the annual ET series.

Figure 4 Variation trend of ET_a in the three parallel rivers basins based on the non-AA (a) annual (b) dry (c) wet, B2015 (d) annual (e) dry (f) wet, and H2018 (g) annual (h) dry (i) wet

Table 3 showed the trends of precipitation and runoff in the three parallel river basins. In terms of precipitation, the increasing magnitude of the precipitation at three temporal scales were 3.2 mm/a, 1.1 mm/a, and 2.6 mm/a, respectively. Runoff in the basins also exhibited increasing trends at three temporal scales, with the magnitude were 2.2 mm/a, 1.2 mm/a, and 1.4 mm/a, respectively. Therefore, the difference between the precipitation variable and the runoff variable on the three temporal scales were 1.0 mm/a, -0.1 mm/a and 1.2 mm/a, respectively. At the same time, synthesizing the inter-annual growth trend of ET_a (1.4 mm/a) in the three parallel river basins, it could be inferred that the difference between precipitation and runoff variables contributed 72% of the ET_a change.

Table 3
Trends of precipitation and runoff in the NRB and LCRB during 1956–2018

Basin		Precipitation			Runoff		
		Annual	Dry	Wet	Annual	Dry	Wet
NRB	NU	2.2	0.7	1.5	3.5	2.2	2.7
	NM	2.9	0.7	2.8	3.2	1.1	2.6
	ND	6.9	2.8	5.3	2.2	1.6	0.9
	Mean	4.0	1.4	3.2	3.0	1.6	2.1
LCRB	LCU	1.5	0.5	1.2	1.8	1.0	1.4
	LCM	4.0	1.2	2.9	1.5	0.4	1.2
	LCD	5.3	2.3	4.5	3.2	1.2	2.1
	Mean	3.6	1.3	2.9	2.2	0.9	1.6
JSRB	JSU	1.0	0.3	0.8	1.6	1.3	0.7
	JSM	2.2	0.9	1.5	1.5	1.1	0.9
	JSD	3.1	1.3	2.1	1.2	1.2	0.8
	Mean	2.1	0.8	1.5	1.4	1.2	0.8

Table 3. Trends of precipitation and runoff in the NRB and LCRB during 1956–2018

In addition, the average increasing magnitude of precipitation in the NRB, LCRB and JSRB were 4.0 mm/a, 3.6 mm/a and 2.1 mm/a, respectively, and the average increasing magnitude of runoff were 3.0 mm/a and 2.2 mm/a, and 1.4 mm/a, respectively. The difference between them were 1.0 mm/a, 1.4 mm/a and 0.7 mm/a, respectively. Based on the variation trend analysis of the ET_a in the NRB (1.41 mm/a), LCRB (1.60 mm/a) and JSRB (1.17 mm /a) in the analysis of the long-term variation trend of the ET_a in the basin, the ratios of the interannual precipitation and runoff variables to the ET_a variables were 0.73, 0.89 and 0.57, respectively. Therefore, according to the theoretical equation of hydrological balance, the precipitation, runoff and ET_a in the NRB and LCRB can basically meet the water closure condition on a long-term scale.

3.3 Influence of meteorological factors on ET_a

Precipitation, temperature and humidity increased from south to north in the three parallel river basins (Fig. 5). On the contrary, wind speed decreased in this direction. The sunshine hours were the shortest in the mid-stream region, which was especially significant in wet season. The precipitation of most stations (25/34) in the three parallel river basins showed an increasing trend, with an average increasing magnitude of 2.4 mm/a. Air temperature in the basins exhibited significant increasing trends at all temporal scales (dry and wet seasons and annual series) during the past 60 years. On the contrary, wind speed showed significant decreasing trends. The variation characteristics of relative humidity also showed a high consistency among three temporal scales at observed stations. In addition, the temporal and spatial trend characteristics of meteorological factors in the dry and wet seasons were basically consistent with the inter-annual trends. Among them, the precipitation, air temperature, relative humidity and sunshine hours in the basin were relatively higher in the wet season, while the wind speed was higher in the dry season. The temporal and spatial changes and seasonal distribution differences between different meteorological factors had a certain degree of positive or negative impact on the ET_a in the basin.

Figure 5 Spatial-temporal variation trend of meteorological factors

The correlation coefficients between meteorological factors and ET_a in the three parallel river basins were shown in Fig. 6 and Fig. 7. There was a positive correlation between ET_a and precipitation, temperature, wind and sunshine hours, with the average cc of 0.40、0.64、0.63 and 0.72, respectively. There was a negative correlation between ET_a and relative humidity in the whole basin, with the average cc of -0.38. The cc values of each meteorological factor in different basins were slightly different. Among them, the temperature and wind speed in the NRB had the strongest correlation with the ET_a, and the average cc were 0.66 and 0.65, respectively. The average cc of precipitation, temperature, wind speed and sunshine hours in the LCRB and ET_a were all higher than 0.60, of which the precipitation has the strongest correlation, with average cc of 0.66. While the sunshine hours in the JSRB had the highest correlation with ET_a, with average cc as high as 0.72.

In addition, the correlation between each meteorological factor and ET_a varies seasonally to a certain extent, and this difference was particularly significant in precipitation and wind speed. The average cc between the dry season precipitation and ET_a was 0.45, which was 0.18 lower than the average cc in the wet season. On the contrary, the correlation between wind speed and ET_a was relatively higher in the dry season. The average cc of each basin was 0.74, which was 0.19 higher than the average value of the cc in the wet season.

Figure 6 The correlations coefficients between meteorological factors and ET_a

Figure 7 The correlations coefficients between meteorological factors and ET_a

The sensitivity coefficient of meteorological factors to ET_a was shown in Table 4. The ET_a in the basins was highly sensitive to temperature, wind speed and sunshine hours, and moderately sensitive to relative humidity. Among them, the NRB had the highest sensitivity coefficient of sunshine hours, with the average sensitivity coefficient of 0.32, while the ET_a in the LCRB was more sensitive to temperature changes, with a sensitivity coefficient of 0.29. The temperature, relative humidity, wind speed and sunshine hours in the JSRB all showed strong sensitivity, and the absolute average sensitivity coefficient fluctuated around 0.25. Moreover, the ET_a was more sensitive to relative humidity and wind speed in the upstream region. Among them, the average values of the sensitivity coefficients of relative humidity and wind speed in the upstream region were − 0.23 and 0.26, respectively.

Table 4
The sensitivity coefficient of meteorological factors on ET_a

Basin		NRB			LCRB			JSRB		
		NU	NM	ND	LCU	LCM	LCD	JSU	JSM	JSD
Temperature	Annual	0.14	0.26	0.25	0.29	0.33	0.26	0.26	0.23	0.33
	Dry	0.04	0.18	0.23	0.25	0.26	0.28	0.22	0.18	0.27
	Wet	0.24	0.34	0.27	0.33	0.40	0.24	0.30	0.28	0.29
	Mean	0.14	0.26	0.25	0.29	0.33	0.26	0.26	0.23	0.30
Relative humidity	Annual	-0.23	-0.14	-0.11	-0.18	-0.15	-0.19	-0.27	-0.20	-0.18
	Dry	-0.25	-0.13	-0.16	-0.23	-0.18	-0.22	-0.24	-0.28	-0.14
	Wet	-0.21	-0.15	-0.06	-0.13	-0.12	-0.16	-0.30	-0.12	-0.22
	Mean	-0.23	-0.14	-0.11	-0.18	-0.15	-0.19	-0.27	-0.20	-0.18
Wind speed	Annual	0.21	0.18	0.14	0.18	0.14	0.17	0.39	0.35	0.14
	Dry	0.24	0.24	0.19	0.27	0.24	0.22	0.30	0.29	0.18
	Wet	0.18	0.12	0.09	0.09	0.04	0.12	0.48	0.41	0.10
	Mean	0.21	0.18	0.14	0.18	0.14	0.17	0.39	0.35	0.14
Sunshine hours	Annual	0.30	0.34	0.32	0.26	0.28	0.14	0.31	0.24	0.20
	Dry	0.35	0.30	0.26	0.31	0.26	0.18	0.29	0.27	0.28
	Wet	0.25	0.38	0.38	0.21	0.30	0.10	0.33	0.21	0.12
	Mean	0.30	0.34	0.32	0.26	0.28	0.14	0.31	0.24	0.20

The sensitivity coefficient between ET_a and meteorological factors had seasonal differences. The difference between the dry season and wet season sensitivity coefficients between ET_a and air temperature, relative humidity and sunshine hours ranges from 0.03 to 0.06. Among them, the difference between the wind speed in the dry season and the wet season was the most significant in each basin, with the average sensitivity coefficient in the dry season of 0.24, indicating that the ET_a was highly sensitive to the change of wind speed in the basin. And the average value of the sensitivity coefficient of the wet season wind speed was 0.18, which was moderately sensitive. In addition, the sensitivity of temperature and sunshine hours in wet season was higher than that in dry season, with the average values of 0.29 and 0.25, respectively.

Table 4. The sensitivity coefficient of meteorological factors on ET_a

4. Discussions

The parameter α is related to the natural characteristics. Researches pointed out that the parameter α in the Priestly-Taylor formula had a wider range of value with roughly 0.6–1.5 (DeBruin 1983; McMahon et al. 2013), which represented the combined effects of the land-atmosphere coupling relationship and underlying vegetation, soil and water conditions on the CR of ET_a. In this study, the value of the parameter α was negatively correlated with the regional aridity index (AI = ET/P) in the basins (Fig. 7), which was consistent with Liu et al. (2016).

Gao et al. (2018) and Zhou et al. (2020) respectively estimated the ET_a distribution in the upstream region of Huaihe river basin and the Loess Plateau based on the generalized complementary principle (B2015 and H2018). The results showed that the simulation accuracy of H2018 was higher than that of B2015 in the Huaihe River basin and the Loess Plateau, and the results are consistent with that in the LCRB and NRB. Gao et al. (2018) pointed out that when α = 1.25, the RE of the method was within ± 5%. Zhou et al. (2020) showed that H2018 and B2015 had the best performance when α = 1.05

and 1.14, respectively. The α value in the basins studied in this paper was relatively low. It is possible that the LCRB and NRB have higher aridity index which is related to the local climatic conditions and vegetation coverage. The developed CR methods after parameter adjustment has good performance in different regions, which provides more references and possibilities for the study of regional ET_a.

ET_a is directly sourced from soil water, open water, and indirectly from water by vegetation (Balugani et al. 2016). Precipitation affects ET_a through soil moisture constraints, especially in arid regions. For example, with high precipitation, ET_a is less limited to soil moisture, and the ET_a might be the same as the potential evapotranspiration (Liu et al. 2012). However, in arid environments with limited precipitation, the soil water content is insufficient, and ET_a tends to be largely dependent on available soil water. The arid environment places a strong constraint on ET_a, causing the ET_a to be much lower than potential evapotranspiration. High temperature accelerates ET_a by providing more energy. And the longer sunshine hours mean that more solar radiation energy is provided. Therefore, ET_a is sensitive to both temperature and sunshine (Li et al. 2017). Wind speed, another meteorological factor positively related to ET_a, is responsible for transporting water heat and carbon dioxide. Wind is in some cases dominating radiation (Liu and Zhang 2013). With an increase in humidity, the moisture content in the air is higher and moisture evaporated into the air decreases (Moratiel et al. 2010). As demonstrated in this study meteorological factors had different effects on ET_a at different time scales in different regions. The quantitative relationship between regional ET_a and climate and soil-plant-atmosphere continuum should be considered in the future.

5. Conclusions

Monthly ET_a in the three parallel river basins were simulated by the hydrological budget balance method based on the observed hydrological and meteorological data from 1956 to 2018. Three generalized complementary functions, non-AA, B2015 and H2018 were evaluated by monthly water-balance-derived values. Impacts of major meteorological factors on ET_a were also assessed. The conclusions were as follows,

(1) All three developed CR methods were able to accurately simulate monthly ET_a series. The relative errors of the monthly ET_a series simulated by the three models were fitted a normal distribution, and the peaks were concentrated in -5%~5%. The NSE between the monthly ET_a simulated by the non-AA, B2015, and H2018 methods and the water-balance-derived values were 0.74, 0.78, and 0.79, respectively. The R-square were 0.84, 0.89, and 0.90, respectively. And the RMSE were 10.76 mm mon^{-1}, 10.01 mm mon^{-1}, and 9.78 mm mon^{-1}, respectively.

(2) The ET_a increased spatially from upstream region to downstream region at catchment scale. The ET_a in the three parallel river basins simulated by the non-AA, B2015 and H2018 models showed an upward trend at all temporal scales (dry and wet seasons and annual series), with the increasing magnitudes of 1.53 mm/a, 1.66 mm/a and 1.47 mm/a, respectively. The precipitation, runoff and ET_a in the basin basically met the water closure condition on a long-term scale.

(3) There was a positive correlation between ET_a and precipitation, temperature, wind and sunshine hours, with the average cc of 0.40、0.64、0.63 and 0.72, respectively. There was a negative correlation between ET_a and relative humidity in the whole basin, with the average correlation coefficients of -0.38. The ET_a in the basins was highly sensitive to temperature, wind speed and sunshine hours, with the average sensitivity coefficient of 0.26, 0.21 and 0.27, respectively. And moderately sensitive to relative humidity, with a sensitivity coefficient of -0.18.

Declarations

Acknowledgements

This study was supported and funded by the Strategic Priority Research Program of the Chinese Academy of Sciences (XDA23090302; XDA2006020202) and the National Natural Science Foundation of China (42171029).

Ethics Approval

Not applicable.

Consent to Participate

Not applicable.

Consent to Publish

Written informed consent for publication was obtained from all participants.

Authors Contributions

All authors contributed to the study conception and design. The first draft of the manuscript was written by Yongshan Jiang and all authors commented on previous versions of the manuscript. All authors read and approved the final manuscript.

Funding

This work was supported and funded by the Strategic Priority Research Program of the Chinese Academy of Sciences (XDA23090302; XDA2006020202) and National Natural Science Foundation of China (42171029).

Competing Interests

We declare that we do not have any commercial or associative interest that represents a conflict of interest in connection with the work submitted.

Availability of Data and Materials

The data and materials used in this study will be made available upon request.

References

1. Allen RG (2000) Using the FAO-56 dual crop coefficient method over an irrigated region as part of an evapotranspiration intercomparison study. J Hydrol 229:27-41. http://doi.org/10.1016/ S0022-1694(99)00194-8.
2. Allen R, Irmak A, Trezza R, Hendrickx JMH, Bastiaanssen W, Kjaersgaard J (2011) Satellite-based ET estimation in agriculture using SEBAL and METRIC. Hydrol Process 25:4011-4027. http://doi.org/10.1002/hyp.8408
3. Balugani E, Lubczynski MW, Metselaar K (2016) A framework for sourcing of evaporation between saturated and unsaturated zone in bare soil condition. Hydrol Sci J 61:1981-1995. http://doi.org/ 10.1080/02626667.2014.966718
4. Bouchet RJ (1963) Evapotranspiration réelle et potentielle, signification climatique. IAHS Publ 62:134-142
5. Brutsaert W (2015) A generalized complementary principle with physical constraints for land surface evaporation. Water Resour Res 51:8087-8093. http://doi.org/10.1002/2015WR017720
6. Brutsaert W, Parlange MB (1998) Hydrologic cycle explains the evaporation paradox. Nature 396:30. http://doi.org/10.1038/23845
7. Brutsaert W, Cheng L, Zhang L (2020) Spatial distribution of global landscape evaporation in the early twenty first century by means of a generalized complementary approach. J Hydrometeorol 21:287-298. http://doi.org/10.1175/JHM-D-19-0208.1
8. Brutsaert W, Li W, Takahashi A, Hiyama T, Zhang L, Liu W (2017) Nonlinear advection-aridity method for landscape evaporation and its application during the growing season in the southern Loess Plateau of the Yellow River basin. Water Resour Res 53:270-282. http://doi.org/ 10.1002/2016WR019472
9. Chen ZJ, Zhu ZC, Jiang H, Sun SJ (2020) Estimating daily reference evapotranspiration based on limited meteorological data using deep learning and classical machine learning methods. J Hydrol 591:125286. http://doi.org/10.1016/j.jhydrol.2020.125286
10. Crago R, Szilagyi J, Qualls R (2016) Rescaling the complementary relationship for land surface evaporation. Water Resour Res 52:8461-8471. http://doi.org/10.1002/2016WR019753
11. DeBruin HAR (1983) A model method for the Priestley-Taylor parameter α. J Clim Appl Meteorol 22:572-578. https://doi.org/10.1175/1520-0450(1983)022<0572:AMFTPT>2.0.CO;2
12. Fan H, He DM (2015) Temperature and precipitation variability and its effects on streamflow in the upstream regions of the Lancang-Mekong and Nu-Salween Rivers. J Hydrometeorol 16:2248-2263. https://doi.org/10.1175/JHM-D-14-0238.1
13. Fan JL, Yue WJ, Wu LF, Zhang FC, Cai HJ, Wang XK, Lu XH, Xiang YZ (2018) Evaluation of SVM, ELM and four tree-based ensemble models for predicting daily reference evapotranspiration using limited meteorological data in different climates of China. Agr Forest Meteorol 263:225-241. https://doi.org/10.1016/j.agrformet.2018.08.019
14. Farahani HJ, Howell TA, Shuttleworth WJ, Bausch WC (2007) Evapotranspiration: Progress in measurement and modeling in agriculture. Trans ASABE 50:1627-1638
15. Fisher JB, Melton F, Middleton E, Hain C, Anderson M, Allen R, Wood EF (2017) The future of evapotranspiration: Global requirements for ecosystem functioning, carbon and climate feedbacks, agricultural management, and water resources. Water Resour Res 53:2618-2626. https://doi.org/10.1002/2016WR020175
16. Gao G, Chen DL, Xu CY, Simelton E (2007) Trend of estimated actual evapotranspiration over China during 1960-2002. J Geophysl Res Atmos 112:D11120. https://doi.org/10.1029/2006JD008010
17. Gao JQ, Qiao M, Qiu XF, Zeng Y, Hua HH, Ye XZ, Adamu M (2018) Estimation of actual evapotranspiration distribution in the Huaihe River upstream basin based on the generalized complementary principle. Adv Meteorol 2018:2158168. https://doi.org/10.1155/2018/2158168
18. Granger RJ, Gray DM (1989) Evaporation from natural nonsaturated surfaces. J Hydrol 111:21-29. https://doi.org/10.1016/0022-1694(89)90249-7
19. Han SJ, Tian FQ (2018) Derivation of a sigmoid generalized complementary function for evaporation with physical constraints. Water Resour Res 54:5050-5068. https://doi.org/10.1029/2017WR021755
20. Han SJ, Hu H, Tian FQ (2008) Evaluating the advection-aridity model of evaporation using data from field-sized surfaces of HEIFE. International Symposium on Flood Forecasting and Water Resource Assessment for IAHS-PUB.
21. Hobbins MT, Ramirez JA, Brown TC, Claessens, LHJM (2001) The complementary relationship in estimation of regional evapotranspiration: The complementary relationship areal evapotranspiration and advection-aridity models. Water Resour Res 37:1367-1387. https://doi.org/10.1029/2000WR900358

22. Jian DN, Li XC, Sun HM, Tao H, Jiang T, Su BD, Hartmann H (2020) Estimation of actual evapotranspiration by the complementary theory-based advection-aridity model in the Tarim River basin, China. J Hydrometeorol 19:289-303. https://doi.org/10.1175/JHM-D-16-0189.1
23. Jiang YS, Liu ZF (2021) Evaluations of Remote Sensing-Based Global Evapotranspiration Datasets at Catchment Scale in Mountain Regions. Remote Sensing, 13, 24:5096. http://10.3390/rs13245096
24. Katul GG, Oren R, Manzoni S, Higgins C, Parlange MB (2012) Evapotranspiration: A process driving mass transport and energy exchange in the soil-plant-atmosphere-climate system. Rev Geophys 50:RG3002. https://doi.org/10.1029/2011RG000366.
25. Li B, Chen F, Liu XM (2017) Sensitivity of the Penman-Monteith reference evapotranspiration to sunshine duration in the upper Mekong River basin. Hydrol Sci J 62:830-842. https://doi.org/ 10.1080/02626667.2016.1243286
26. Li XP, Wang L, Chen DL, Yang K, Wang AH (2014) Seasonal evapotranspiration changes (1983–2006) of four large basins on the Tibetan Plateau. J Geophys Res 119:13079-13095. https://doi.org/10.1002/2014JD022380
27. Liu Z, Yao Z, Huang H, Wu S, Liu G (2014) Land use and climate changes and their impacts on runoff in the Yarlung Zangbo River basin, China. Land Degrad Dev 25:203-215. https://doi.org/10.1002/ldr.1159
28. Liu M, Bardossy A, Li J (2012) Physically-based modeling of topographic effects on spatial evapotranspiration and soil moisture patterns through radiation and wind. Hydrol Earth Syst Sci 16:357-373. https://doi.org/10.5194/hess-16-357-2012
29. Liu WB, Wang L, Zhou J, Li YZ, Sun FB, Fu GB, Li XP, Sang YF (2016) A worldwide evaluation of basin-scale evapotranspiration estimates against the water balance method. J Hydrol 538:82-95. https://doi.org/10.1016/j.jhydrol.2016.04.006
30. Liu XM, Zhang D (2013) Trend analysis of reference evapotranspiration in Northwest China: The roles of changing wind speed and surface air temperature. Hydrol Process 27:3941-3948. https://doi.org/10.1002/hyp.9527
31. Liu XM, Liu CM, Brutsaert W (2016) Regional evaporation estimates in the eastern monsoon region of China: Assessment of a nonlinear formulation of the complementary principle. Water Resour Res 52:9511-9521. https://doi.org/10.1002/2016WR019340
32. Liu Z, Yao Z, Wang R (2019) Simulation and evaluation of actual evapotranspiration based on inverse hydrological modeling at a basin scale. Catena 180:160-168. https://doi.org/10.1016/j.catena.2019.03.039
33. Li Z, Chen YN, Yang J, Wang Y (2014) Potential evapotranspiration and its attribution over the past 50 years in the arid region of Northwest China. Hydrol Process 28:1025-1031. https://doi.org/10.1016/10.1002/hyp.9643
34. Ma N, Szilagyi J (2019) The CR of evaporation: A calibration-free diagnostic and benchmarking tool for large-scale terrestrial evapotranspiration modeling. Water Resour Res 55:7246-7274. https://doi.org/10.1029/2019WR024867
35. Maes WH, Steppe K (2012) Estimating evapotranspiration and drought stress with ground-based thermal remote sensing in agriculture: a review. J Exp Bot 63:4671-4712. https://doi.org/10.1093/jxb/ers165
36. Masson V, Champeaux JL, Chauvin F, Meriguet C, Lacaze R (2003) A global database of land surface parameters at 1km resolution in meteorological and climate models. J Clim 9:1261-1282. https://doi.org/10.1175/1520-0442-16.9.1261
37. McCuen RH (1974) A sensitivity and error analysis of procedures used for estimating evaporation. J AM Water Resour Assoc 10:486-497. https://doi.org/10.1111/j.1752-1688.1974.tb00590.x
38. McMahon TA, Peel MC, Lowe L, Srikanthan R, McVicar TR (2013) Estimating actual, potential, reference crop and pan evaporation using standard meteorological data: A pragmatic synthesis, Hydrol Earth Syst Sci 17:1331-1363. https://doi.org/10.5194/hess-17-4503-2013
39. Moratiel R, Duran JM, Snyder RL (2010) Responses of reference evapotranspiration to changes in atmospheric humidity and air temperature in Spain. Clim Res 44:27-40. https://doi.org/ 10.3354/cr00919
40. Morton FI (1983) Operational estimates of areal evapotranspiration and their significance to the science and practice of hydrology. J Hydrol 66:1-76. https://doi.org/10.1016/0022-1694(83)90177-4
41. Oki T, Kanae S (2006) Global hydrological cycles and world water resources. Science 313:1068-1072. https://doi.org/10.1126/science.1128845
42. Penman HL (1948) Natural evaporation from open water, bare soil and grass. Proc R Soc Lond A Math Phys Sci 193:120-145. https://doi.org/10.1098/rspa.1948.0037
43. Priestley CHB, Taylor RJ (1972) On the assessment of surface heat flux and evaporation using large-scale parameters. Mon Weather Rev 100:81-92. https://doi.org/10.1175/1520-0493(1972)1002.3.CO;2
44. Sabo JL, Ruhi A, Holtgrieve GW, Elliott V, Arias ME, Ngor PB, Rasanen TA, Nam S (2017) Designing river flows to improve food security futures in the Lower Mekong Basin. Science 358: eaao1053. https://doi.org/10.1126/science.aao1053
45. Szilagyi J (2007) On the inherent asymmetric nature of the complementary relationship of evaporation. Geophys Res Lett 34:L02405. https://doi.org/10.1029/2006GL028708
46. Szilagyi J, Crago R, Qualls R (2017) A calibration-free formulation of the complementary relationship of evaporation for continental-scale hydrology. J Geophys Res 122:264-278. https://doi.org/ 10.1002/2016JD025611
47. Szilagyi J, Hobbins MT, Jozsa J (2009) Modified advection-aridity model of evapotranspiration. J Hydrol Eng 14:569-574. https://doi.org/10.1061/(ASCE)HE.1943-5584.0000026
48. Trenberth KE, Fasullo JT, Kiehl J (2009) Earth's global energy budget. Bull AM Meteorol Soc 90:311-323. https://doi.org/10.1175/2008BAMS2634.1

49. Valipour M (2015) Importance of solar radiation, temperature, relative humidity, and wind speed for calculation of reference evapotranspiration. Arch Agron Soil Sci 61:239-255. https://doi.org/10.1080/03650340.2014.925107
50. Wan ZM, Zhang K, Xue XW, Hong Z, Hong Y, Gourley JJ (2015) Water balance based actual evapotranspiration reconstruction from ground and satellite observations over the Conterminous United States. Water Resour Res 51:6485-6499. https://doi.org/10.1002/2015WR017311
51. Xu CY, Singh VP (2005) Evaluation of three complementary relationship evapotranspiration models by water balance approach to estimate actual regional evapotranspiration in different climatic regions. J Hydrol 308:104-121. https://doi.org/10.1016/j.jhydrol.2004.10.024
52. Xu RR, Gao P, Mu XM, Gu CJ (2021) Spatial-temporal change of actual evapotranspiration and the causes based on the advection-aridity model in the Weihe River basin, China. Water 13:303. https://doi.org/10.3390/w13030303
53. Yang JH, Wang W, Hua TT, Peng M (2021) Spatiotemporal variation of actual evapotranspiration and its response to changes of major meteorological factors over China using multi-source data. J Water Clim Change 12:325-338. https://doi.org/10.2166/wcc.2020.221
54. Zhang L, Cheng L, Brutsaert W (2017) Estimation of land surface evaporation using a generalized nonlinear complementary relationship. J Geophys Res 122:1475-1487. https://doi.org/ 10.1002/2016JD025936
55. Zhang YQ, Leuning R, Chiew FHS, Wang EL, Zhang L, Liu CM, Sun FB, Peel MC, Shen YJ, Jung M (2012) Decadal trends in evaporation from global energy and water balances. J Hydrometeorol 13:379-391. https://doi.org/10.1175/JHM-D-11-012.1
56. Zhou HX, Han SJ, Liu WZ (2020) Evaluation of two generalized complementary functions for annual evaporation estimation on the Loess Plateau, China. J Hydrol 587:124980. https://doi.org/10.1016/j.jhydrol.2020.124980

Figures

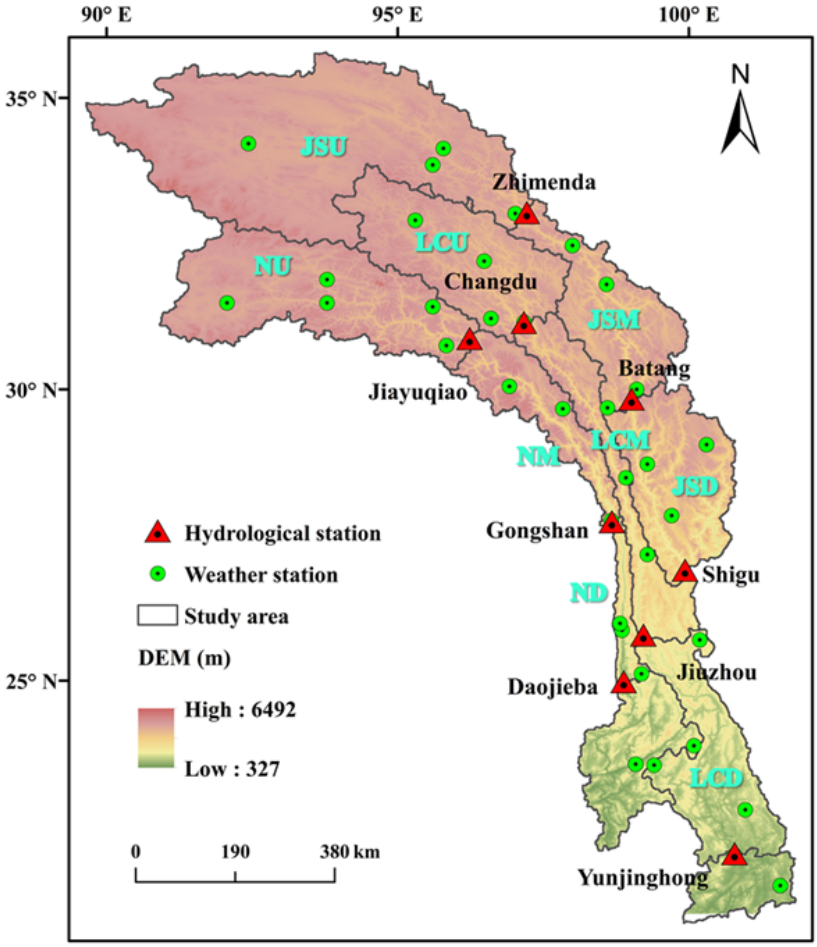

Figure 1

Location of each catchment, hydrological stations, and weather stations (The catchment was defined by hydrological stations in the main stream. The NU, NM, and ND represented the upstream, mid-stream, and downstream regions of Nu River basin respectively. The LCU, LCM, and LCD represented the upstream, midstream, and downstream regions of Lancang River basin respectively. The JSU, JSM, and JSD represented the upstream, midstream, and downstream regions of Jinsha River basin respectively)

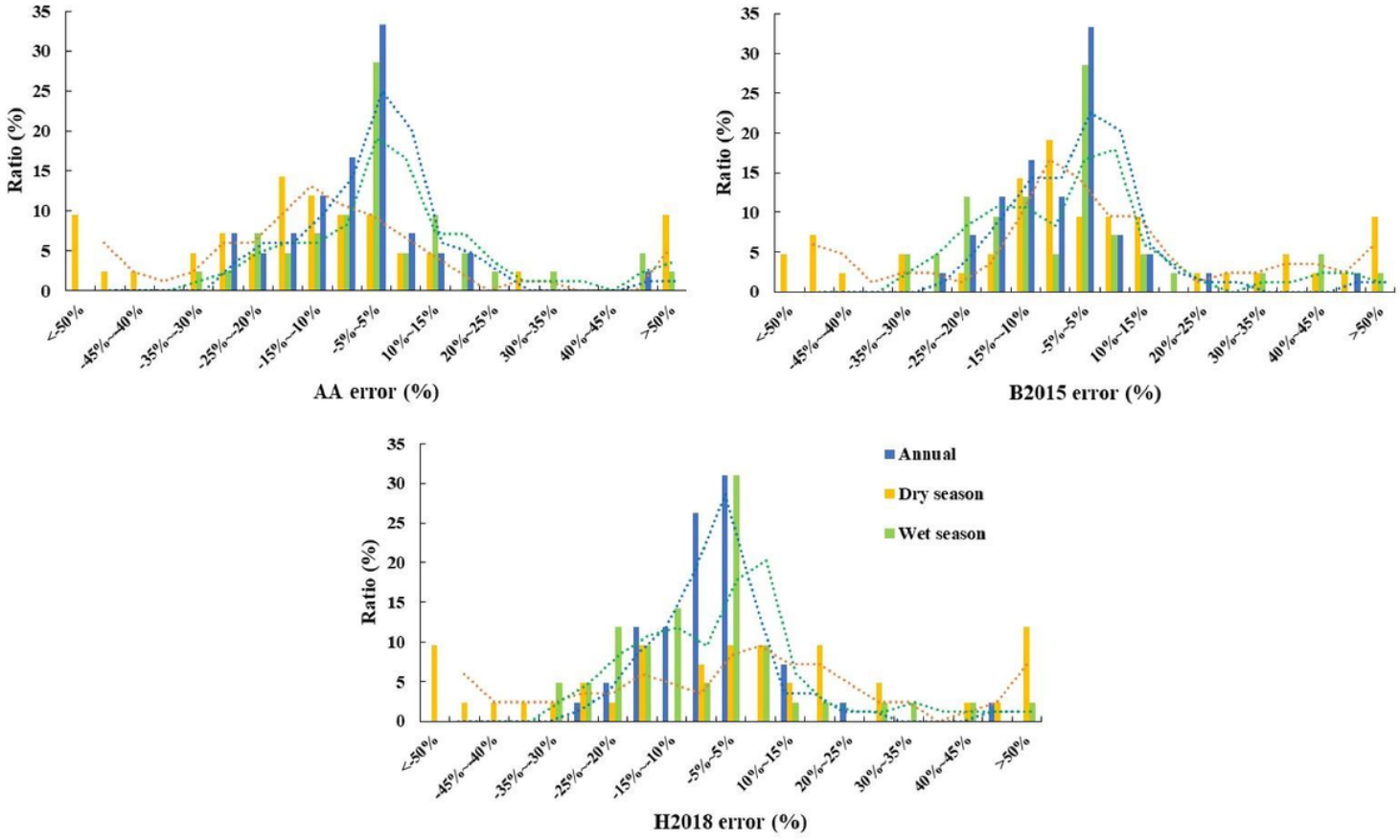

Figure 2

Frequency distributions of the relative error for the non-AA, B2015 and H2018 methods

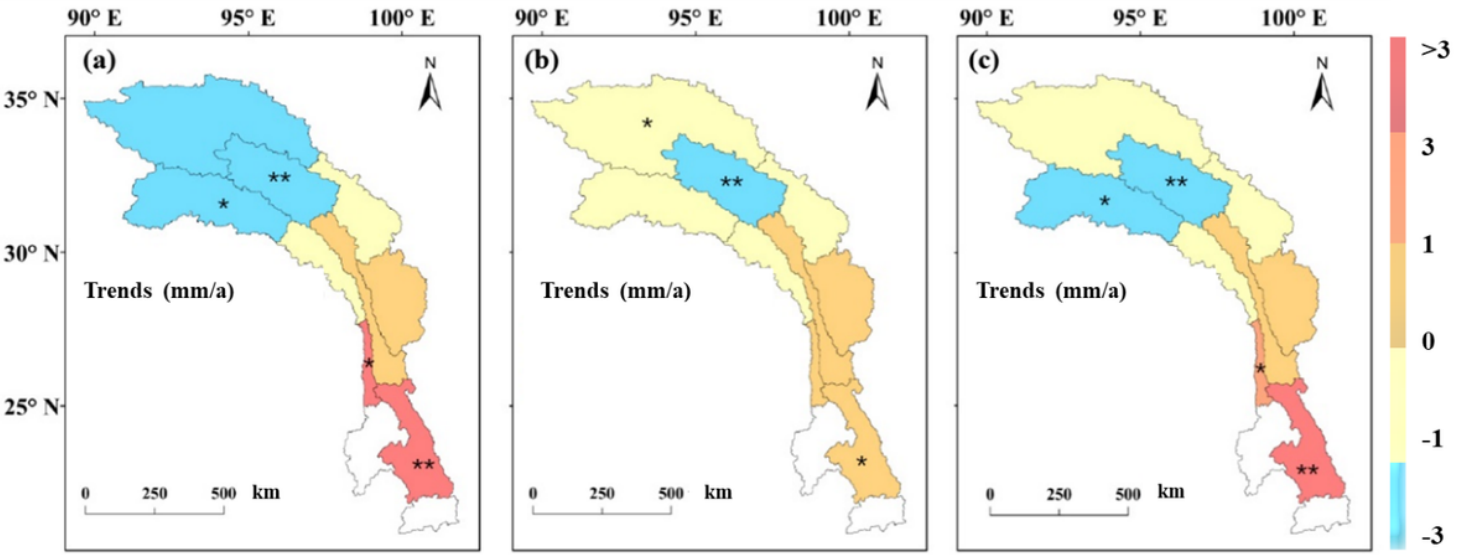

Figure 3

Variation trend of ET_a of (a) interannual (b) dry season (c) wet season in the three parallel rivers region basins (* represents significance level of 0.05, ** represents significance level of 0.01)

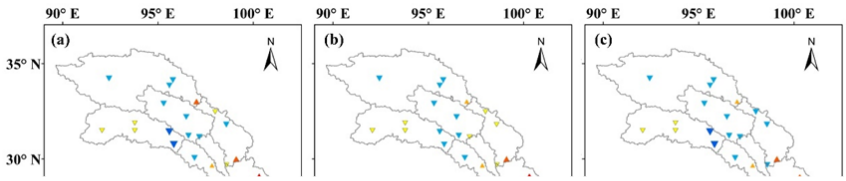

Figure 4

Variation trend of ET_a in the three parallel rivers basins based on the non-AA (a) annual (b) dry (c) wet, B2015 (d) annual (e) dry (f) wet, and H2018 (g) annual (h) dry (i) wet (Red/Orange triangles represent increase trends, and blue triangles are decreasing trends. Large symbols indicate the significance level of 0.05)

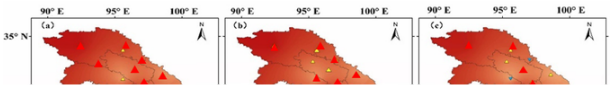

Figure 5

Spatial-temporal variation trend of meteorological factors

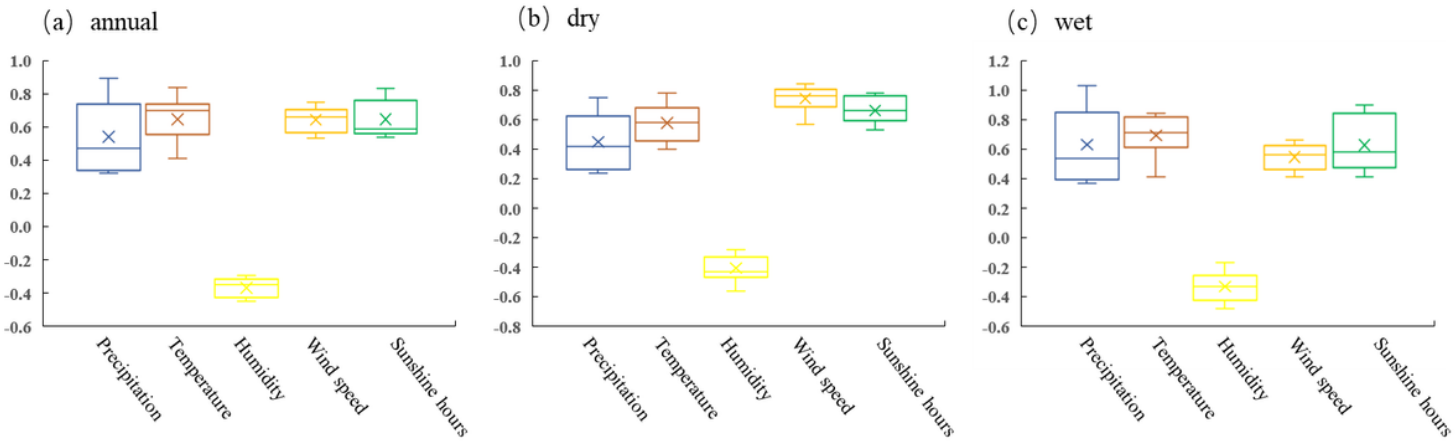

Figure 6

The correlations coefficients between meteorological factors and ET_a

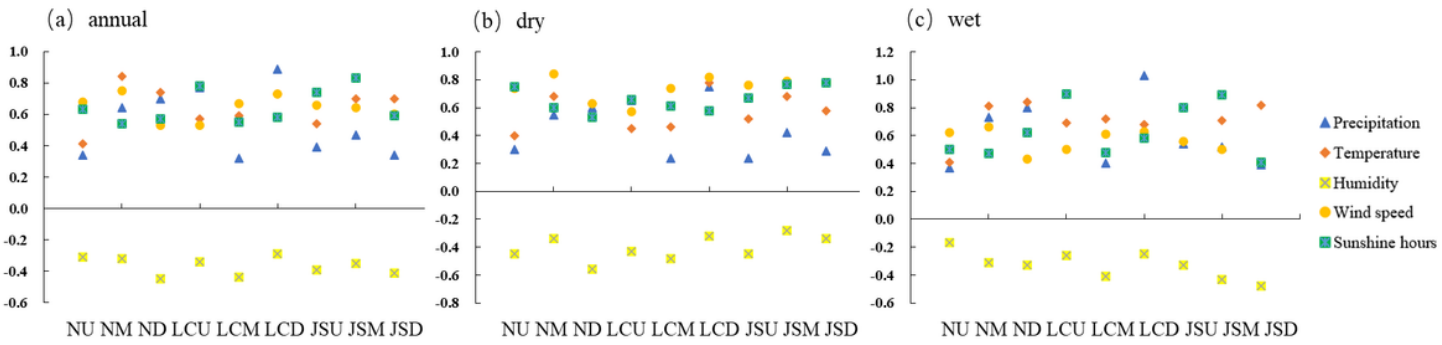

Figure 7

The correlations coefficients between meteorological factors and ET_a